JOURNAL OF PHYSICAL ORGANIC CHEMISTRY
J. Phys. Org. Chem. 2005; **18:** 90–95
Published online 21 September 2004 in Wiley InterScience (www.interscience.wiley.com). DOI: 10.1002/poc.860

Dynamics and reactivity of chiral ion–dipole pairs†

Maurizio Speranza*

Dipartimento di Studi di Chimica e Tecnologia delle Sostanze Biologicamente Attive, Università degli Studi di Roma 'La Sapienza', P.le A. Moro 5, 00185 Rome, Italy

Received 26 September 2003; revised 2 April 2004; accepted 4 March 2004

ABSTRACT: Modeling ionic reactions in a dynamic environment, such as in a solvent cage, requires the generation of tailor-made ionic adducts involved in the process and the investigation of the intrinsic structural and electronic factors governing their behavior in the unsolvated state. A compendium of the most recent studies on the gas-phase dynamics and reactivity of chiral ion–dipole pairs involved in classical organic reactions is reported, together with a presentation of the experimental and theoretical methodologies adopted. Copyright © 2004 John Wiley & Sons, Ltd.

KEYWORDS: ion–dipole complexes; gas-phase dynamics and reactivity; chiral ions; radiolysis; racemization

INTRODUCTION

Ion–neutral complexes (INC) in the gas phase may represent ideal systems for modeling the behavior of ions in a dynamic environment, such as the solvent cage in solution. Many tailor-made ICN can be readily generated in the isolated state by mass spectrometric methods and the intrinsic factors governing their dynamics and reactivity determined. Comparing the behavior of the same ion in the gaseous and condensed phase provides valuable information on how these factors are sensitive to solvation and ion pairing phenomena.[1–4] Obviously, to stand comparison with thermal kinetics in solution, the evolution of the ICN to products in the isolated state must be in constant thermal equilibrium with the missing reaction medium. A reasonable compromise to settle this evident contradiction is to generate the INC in a large excess of an inert gaseous medium at pressures low enough to avoid the formation of organized ionic clusters, yet sufficiently high to allow collisional thermalization of the unsolvated reaction intermediates well before their conversion to products. A consolidated kinetic methodology fulfilling these conditions is based on the production of the ionic reactants at atmospheric pressures by γ-radiolysis.[5]

The study of INC in the isolated state also extends to their stereochemistry. Intracomplex reactions generally involve the rearrangement of the reactants or simply their mutual reorientation before reaction or dissociation. Thus, the knowledge of the structure, the configuration and the initial orientation of the INC components is crucial for understanding their stereochemistry in the gas phase. A distinctive feature of the radiolytic method is that ion–dipole reactivity can be evaluated by standard kinetic procedures and their regio- and stereochemistry assessed by the actual isolation and structural discrimination of the relevant reaction products. These basic features, coupled with the possibility of operating under thermal conditions, confer upon radiolysis a role in gas-phase ion chemistry complementary to that covered by mass spectrometry, in which thermalization of ionic transients is prevented by the low-pressure operating regime and their structural characterization severely hampered by the inadequacy of technique to discriminate among isomeric species.[5]

A survey of the most recent applications of the radiolytic approach to the gas-phase study of classical ionic reactions, such as acid-induced isomerization of chiral *sec*-butyl ion–toluene pairs (Scheme 1)[6] and racemization of chiral α-methylbenzyl cation–methanol adducts (Scheme 2),[7] is provided in this paper. It is hoped thereby to provide a much sharper view of these classical reactions.

EXPERIMENTAL

Chiral *sec*-butyl ion–toluene complexes

Gaseous mixtures were prepared by conventional procedures with the use of a greaseless vacuum line. A chiral *sec*-butyl ion–toluene complex was obtained in the gas phase [60 Torr (1 Torr = 133.3 Pa); 100–160 °C] by protonating the starting arene $\mathbf{1_S}$ [or its analogue (±)-2-(*p*-[D_7]tolyl)butane $\mathbf{1^D}$] with radiolytically formed $C_nH_5^+$

**Correspondence to:* M. Speranza, Dipartimento di Studi di Chimica e Tecnologia delle Sostanze Biologicamente Attive, Università degli Studi di Roma 'La Sapienza', P.le A. Moro 5, 00185 Rome, Italy.
E-mail: maurizio.speranza@uniroma1.it

†Selected article presented at the Seventh Latin American Conference on Physical Organic Chemistry (CLAFQO-7), 21–26 September 2003, Florianópolis, Brazil.

Contract/grant sponsors: Ministero della Università e della Ricerca Scientifica e Tecnologica (MURST); Consiglio Nazionale delle Ricerche (CNR).

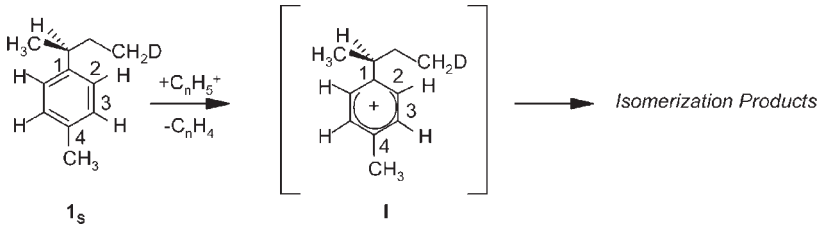

Scheme 1

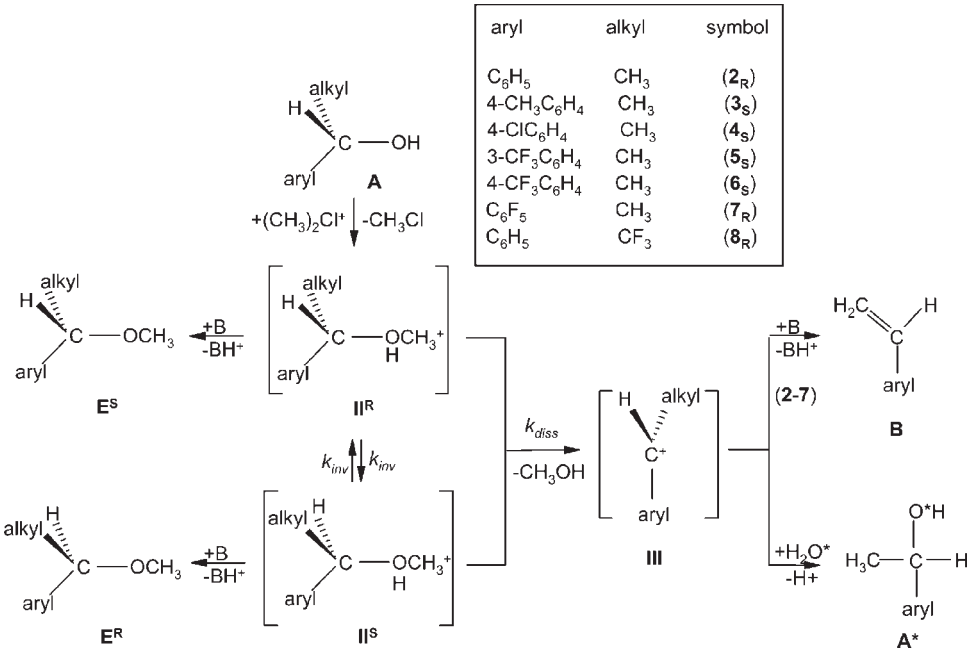

Scheme 2

(or $C_nD_5^+$) ($n = 1, 2$), in the presence of a thermal radical scavenger (O_2; 10 Torr) and a powerful base [$(C_2H_5)_3N$; 0.1 Torr]. The radiolytic products were analyzed by enantioselective HRGC–MS. The product yields were determined from the areas of the corresponding eluted peaks, using an internal standard (acetophenone) and individual calibration factors to correct for the detector response. Control experiments were carried out to rule out the occurrence of thermal fragmentation, isomerization and racemization of the starting arene and of their isomeric products within the temperature range investigated.

The D content and location in the radiolytic products were determined by HRGC–MS, setting the mass analyzer in the selected ion monitoring (SIM) mode. The ion fragments at *m/z* 119 ($[M - C_2H_4D]^+$), 120 ($[M - C_2H_5]^+$), and 149 ($M^{+\cdot}$) were monitored to analyze all the GC-separated isomers of $\mathbf{1_S}$ ($= M$). The isomers of $\mathbf{1^D}$ ($= M^D$) were examined by using the fragments at *m/z* 125 ($[M^D - C_2H_4D]^+$), 126 ($[M^D - C_2H_5]$) and 155 ($M^{D+\cdot}$). Toluenes, obtained from $\mathbf{1_S}$ and $\mathbf{1^D}$, were analyzed by monitoring the ions at *m/z* 91–93 and 96–100, respectively.

Chiral α-methylbenzyl cation–methanol complexes

The methods of preparation, irradiation and analysis of the gaseous mixtures were described in the previous section. Ring-substituted α-methylbenzyl cation–methanol complexes were obtained in the gas phase (720 Torr; 25–160 °C) by methylating the starting chiral alcohol [e.g. **A**; aryl;alkyl = C_6H_5;CH_3 ($\mathbf{2_R}$), 4-$CH_3C_6H_4$;CH_3 ($\mathbf{3_S}$), 4-ClC_6H_4;CH_3 ($\mathbf{4_S}$), 3-$CF_3C_6H_4$;CH_3 ($\mathbf{5_S}$), 4-$CF_3C_6H_4$;CH_3 ($\mathbf{6_S}$), C_6F_5:CH_3 ($\mathbf{7_R}$), and C_6H_5:CF_3 ($\mathbf{8_R}$)] with dimethylchloronium ions, $(CH_3)_2Cl^+$, generated by γ-radiolysis of CH_3Cl, in the presence of $H_2{}^{18}O$ (2–3 Torr), the radical scavenger O_2 (4 Torr) and the powerful base B = $(C_2H_5)_3N$ (0.2–1.2 Torr).[6] The radiolytic products were analyzed by enantioselective HRGC, with a Perkin-Elmer 8700 gas chromatograph equipped with a flame ionization detector, on the same columns as used to analyze the starting alcohols.

The extent of ^{18}O incorporation into the radiolytic products was determined by HRGC–MS, setting the mass analyzer in the SIM mode. The ion fragments corresponding to ^{16}O-$[M - CH_3]^+$ and ^{18}O-$[M - CH_3]^+$

(M^+ = parent ion) were monitored to analyze alcohols **A*** and their methylated ethers **E**. The ion fragments corresponding to $^{16}O\text{-}[M]^+$ and $^{18}O\text{-}[M]^+$ were monitored to analyze alcohols **8**, and the extent of labeling of its methylated ethers **E** was measured by using the corresponding $^{16}O\text{-}[M - CF_3]^+$ and $^{18}O\text{-}[M - CF_3]^+$ fragments.

RESULTS AND DISCUSSION

Chiral *sec*-butyl ion–toluene complexes

Ring-protonated (*S*)-(+)-1-D_1-3-(*p*-tolyl)butane **I** was generated by attack of radiolytic $C_nH_5^+$ ($n = 1, 2$) ions on (*S*)-(+)-1-D_1-3-(*p*-tolyl)butane $\mathbf{1_S}$ and its isomerization kinetics and stereochemistry investigated in the gas phase at 70 Torr and 100–160 °C (Scheme 1).[6] The process leads to the exclusive formation of the relevant *meta* isomer with complete racemization and partial 1, 2-H shift in the migrating 2-butyl group. These results, together with the relevant activation parameters [$\Delta H^* = 10.3 \pm 1.2$ kcal mol^{-1}; $\Delta S^* = -5.3 \pm 3.6$ cal mol^{-1} K^{-1} (1 cal = 4.184 J)], point to the occurrence of tightly bound, isomeric 2-butyl ion–toluene complexes of defined structure and stability situated ca 10 kcal mol^{-1} below the classical electrostatically bound π-complexes on the relevant potential energy surface (PES). The existence and the η^1-type structure of these low-energy intermediates are confirmed by *ab initio* calculations (Fig. 1).

Formation of the tightly bound η^1-type complexes in the isomerization of **I** raises some questions about the role of these intermediates in determining the substrate and positional selectivity of the gas-phase ionic alkylation of arenes. Indeed, the classical mechanistic model of gas-phase aromatic alkylations involves the preliminary formation of an electrostatically bound π-complex acting as a microscopic reaction 'vessel' wherein the reactants are confined by electrostatic forces. The substrate selectivity of the alkylation reaction essentially reflects the competition between the collisional stabilization of the individual π-complexes and their back-dissociation. The positional selectivity reflects instead the different activation free energies for the conversion of the π-complex to isomeric σ-bonded arenium ions.

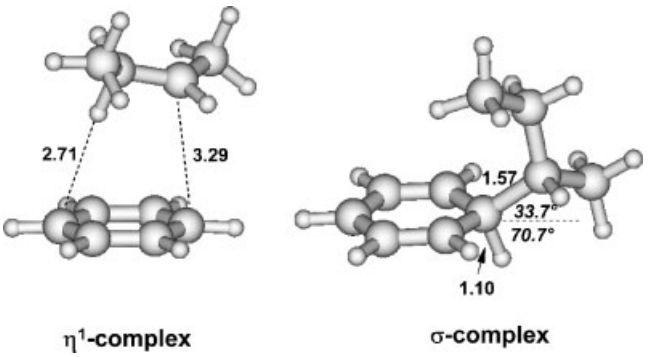

Figure 1. HF/6–31 + G**-optimized structures and main geometric parameters of the stable σ- and η^1-type complexes located on the potential energy surface (PES) of **I** [bond lengths in Å; angles in degrees (in italics)]

The discovery of tightly bound, isomeric η^1-type complexes on the 2-butyl ion–toluene PES challenges this widely accepted model. Indeed, their occurrence provide a rationale for the significant pressure effect on the isomeric product pattern observed in the gas-phase *sec*-butylation of toluene (24 °C).[8] This pressure effect can be explained only by acknowledging the intermediacy of isomeric η^1-type complexes with lifetimes comparable to their collision time with the bulk gas at 70–710 Torr (5×10^{-10}–5×10^{-11} s).

In this frame, the positional selectivity of the gas-phase *sec*-butylation of toluene, a model reaction for electrophilic aromatic substitutions, is determined by the relative population of isomeric η^1-type complexes and the activation free energies for their conversion to the relevant σ-bonded arenium ions. When collisional cooling of the η^1-type complexes is efficient (high pressure), the reaction is essentially controlled by enthalpy factors favoring the formation of their *ortho* and *para* isomers and their conversion to the corresponding σ-arenium intermediates. When instead collisional cooling of the η^1-type complexes is not so efficient (low pressure), their relative population and conversion to the corresponding σ-arenium ion can be significantly altered by the contribution of the entropic factors.

Chiral α-methylbenzyl cation–methanol complexes

Detailed information on the reorganization dynamics of the intimate ion–dipole pair arising from C—O bond cleavage in a family of enantiomerically pure oxonium ions **II** (Scheme 2) is inferred from a detailed kinetic study of their inversion of configuration and dissociation to α-methylbenzyl cation (**III**) and CH_3OH.[7] The oxonium ions **II** were generated in the gas phase by $(CH_3)_2Cl^+$ methylation of the corresponding 1-arylethanols. Figures 2 and 3 report the Arrhenius plots of k_{inv} and k_{diss}, respectively, for all the selected alcohols **2**–**8**. The relevant linear curves obey the equations reported in Tables 1 and 2, respectively. The corresponding activation parameters were calculated from the transition-state theory.

The activation parameters of the inversion reaction are found to obey two different isokinetic relationships (IKR) depending on the nature and position of the substituents in the oxonium ions **II**. In contrast, the activation parameters of the dissociation reaction obey a single isokinetic relationship. The curves in Fig. 4 show the existence of two different enthalpy–entropy compensation effects

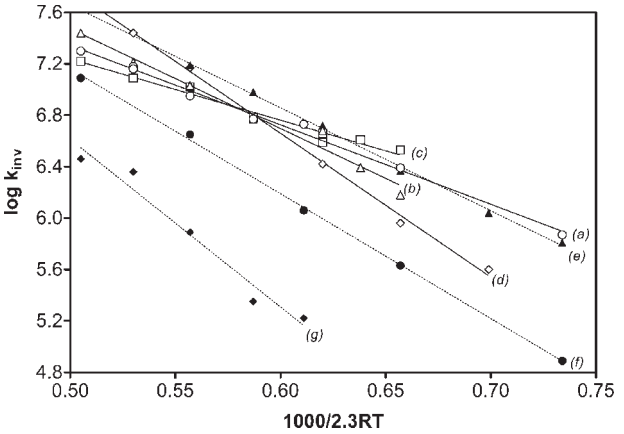

Figure 2. Arrhenius plots for the inversion of configuration of the oxonium ions **II** from **2** (a), **3** (b), **4** (c) and **5** (d) (the F family) and from **6** (e), **7** (f) and **8** (g) (the G family)

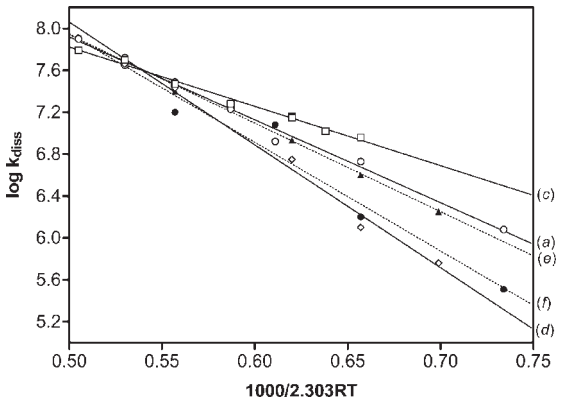

Figure 3. Arrhenius plots for the dissociation of the oxonium ions **II** from **2** (a), **4** (c), **5** (d), **6** (e), and **7** (f) (the E family)

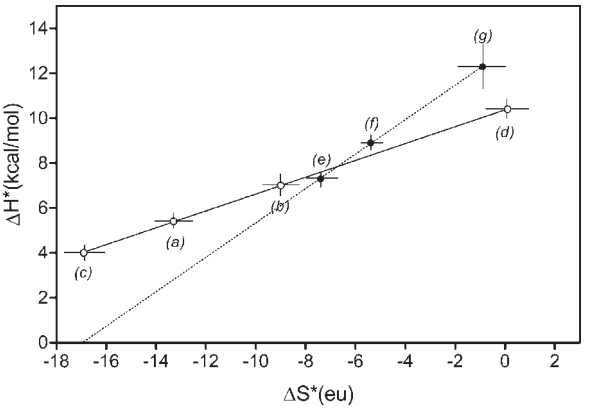

Figure 4. Enthalpy–entropy compensation plots for the inversion of **II** from **2** (a), **3** (b), **4** (c) and **5** (d) (the F family) and from **6** (e), **7** (f) and **8** (g) (the G family)

on the gas-phase inversion of the oxonium ions **II** related to the nature of their precursors, i.e. the F family (**2**–**5**) and the G family (**6**–**8**). In contrast, the curve in Fig. 5 points to the existence of a single enthalpy–entropy compensation in the gas-phase dissociation of the same ions, i.e. the E family (**2**, **4**, **5**, **6** and **7**).

The definition of IKR implies that, at the isokinetic temperature (T_{iso}), $\Delta G^*_{iso} = \Delta H^* - T_{iso}\Delta S^* = \text{constant}$. Therefore, the slopes of the linear curves in Figs. 4 and 5 provide the relevant T_{iso} values and the y-intercepts give an estimate of the corresponding ΔG^*_{iso} terms. Accordingly, the isokinetic parameters for the F inversion reactions are $T_{iso} = 376 \pm 2\,K$, $\Delta G^*_{iso} = 10.37 \pm 0.02\,kcal\,mol^{-1}$ and $\log k_{iso} = 6.84$, whereas those for the G inversion reactions are $T_{iso} = 767 \pm 10\,K$, $\Delta G^*_{iso} = 13.00 \pm 0.05\,kcal\,mol^{-1}$ and $\log k_{iso} = 9.35$. Similarly,

Table 1. Arrhenius parameters for the gas-phase inversion of configuration of oxonium ions **II**

Precursor of oxonium ion **II**	Arrhenius equation ($y = 1000/2.303RT$)	Correlation coefficient (r^2)	ΔH^*_{inv} (kcal mol^{-1})	ΔS^*_{inv} (cal mol^{-1} K^{-1})
$\mathbf{2_R}$	$\text{Log}\,k_{inv} = (10.4 \pm 0.1) - (6.2 \pm 0.2)y$	0.994	5.4 ± 0.3	-13.3 ± 1.0
$\mathbf{3_S}$	$\text{Log}\,k_{inv} = (11.3 \pm 0.3) - (7.8 \pm 0.5)y$	0.978	7.0 ± 0.5	-9.0 ± 0.9
$\mathbf{4_S}$	$\text{Log}\,k_{inv} = (9.6 \pm 0.2) - (4.8 \pm 0.3)y$	0.973	4.0 ± 0.4	-16.9 ± 0.9
$\mathbf{5_S}$	$\text{Log}\,k_{inv} = (13.3 \pm 0.2) - (11.1 \pm 0.3)y$	0.997	10.4 ± 0.3	$+0.1 \pm 1.1$
$\mathbf{6_S}$	$\text{Log}\,k_{inv} = (11.7 \pm 0.1) - (8.0 \pm 0.2)y$	0.998	7.3 ± 0.3	-7.4 ± 0.8
$\mathbf{7_R}$	$\text{Log}\,k_{inv} = (12.0 \pm 0.1) - (9.7 \pm 0.2)y$	0.999	8.9 ± 0.2	-5.4 ± 0.5
$\mathbf{8_R}$	$\text{Log}\,k_{inv} = (13.1 \pm 0.8) - (13.0 \pm 1.5)y$	0.964	12.3 ± 1.5	-0.9 ± 1.0

Table 2. Arrhenius parameters for the gas-phase dissociation of oxonium ions **II** to benzyl cations **III** and methanol

Precursor of oxonium ion **II**	Arrhenius equation ($y = 1000/2.303RT$)	Correlation coefficient (r^2)	ΔH^*_{diss} (kcal mol^{-1})	ΔS^*_{diss} (cal mol^{-1} K^{-1})
$\mathbf{2_R}$	$\text{Log}\,k_{diss} = (11.9 \pm 0.3) - (7.9 \pm 0.2)y$	0.992	7.1 ± 0.3	-6.7 ± 1.2
$\mathbf{4_S}$	$\text{Log}\,k_{diss} = (10.6 \pm 0.1) - (5.7 \pm 0.2)y$	0.989	4.9 ± 0.3	-12.2 ± 0.7
$\mathbf{5_S}$	$\text{Log}\,k_{diss} = (13.9 \pm 0.4) - (11.7 \pm 0.7)y$	0.990	10.9 ± 0.6	$+2.6 \pm 2.0$
$\mathbf{6_S}$	$\text{Log}\,k_{diss} = (12.1 \pm 0.3) - (8.4 \pm 0.5)y$	0.990	7.7 ± 0.5	-5.4 ± 1.4
$\mathbf{7_R}$	$\text{Log}\,k_{diss} = (13.1 \pm 0.7) - (10.3 \pm 1.1)y$	0.965	9.6 ± 1.1	-0.9 ± 1.9

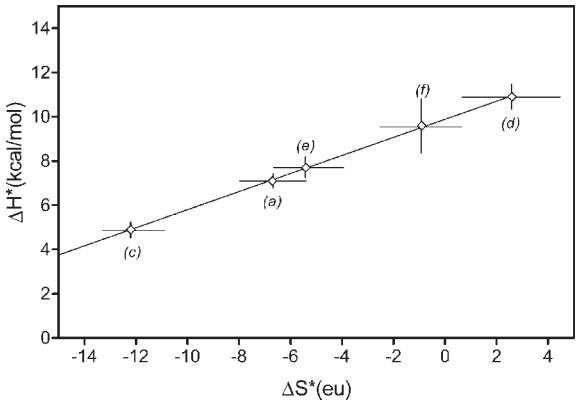

Figure 5. Enthalpy–entropy compensation plot for the dissociation of **II** from **2** (a), **4** (c), **5** (d), **6** (e) and **7** (f) (the E family)

the isokinetic parameters for the E dissociations are $T_{iso} = 409 \pm 5\,K$, $\Delta G^*_{iso} = 9.89 \pm 0.04\,kcal\,mol^{-1}$ and $\log k_{iso} = 7.61$.

The origin of IKR can be interpreted in terms of Linert's model.[9] The rate constant of a given reaction taking place in a constant-temperature 'heat bath' (HB) depends on the collision number between the reacting system (M) and HB molecules, the energy barrier height of the given process, the temperature of the 'heat bath' and the quantum-mechanical transition probability between any reactant level and the transition structure. When the 'heat bath' contains energy stored in the form of vibrational degrees, the transition probabilities for vibrational–vibrational energy transfer is expressed by $P_{l,m} = l\exp(\omega/\nu)$ (where m is the HB vibrational level associated with ν and l is that associated with M) and reach the maximum value for a resonant vibrational–vibrational coupling, i.e. when $\nu m = \omega l$. In the condensed phase, cooperative supramolecular effects normally make available HB vibrational frequency gaps ($\Delta\nu$) which are much smaller than those of M ($\Delta\omega$). In this case, the only variable parameter for a family of reactions is ω and, therefore, the IKR can be expressed mathematically as $d\ln k(\omega)/d\omega = 0$ at T_{iso}. Accordingly, for a homogeneous family of reactions, such as the **II** inversion, a single T_{iso} should be expected whose value (in kelvin) is related to the characteristic vibrational frequency ν (in cm^{-1}) predominantly exchanging energy in HB by the $T_{iso} = h\nu/2k_B$ equation, where k_B = Botzmann's constant and h = Planck's constant.

Although this is the case for the gas-phase E dissociation (Figs 3 and 5), the observation in the same gaseous HB (CH_3Cl at 720 Torr) of two isokinetic temperatures for **II** inversion (Figs 2 and 4) underlines the existence of a point of discontinuity in the ν–ω coupling which may be peculiar for gaseous media where cooperative supramolecular effects are negligible and, hence, the variable parameters for a family of reactions are both ν and ω.[9]

In this frame, the two IKR of Fig. 2 can be rationalized in terms of Larsson's selective energy transfer (SET) model,[10] which introduces in Linert's model the notion of possible switchovers in the resonant ν–ω coupling. Thus, with the assumption of full ν–ω resonance ($T_{iso} = h\nu/2k_B$), $T_{iso} = 376 \pm 2\,K$ for the inversion of configuration of the F family corresponds to a vibrational frequency ν_F predominantly exchanging energy of $523 \pm 3\,cm^{-1}$, while $T_{iso} = 767 \pm 10\,K$ for the inversion of the G family to a predominant vibrational frequency $\nu_G = 1067 \pm 14\,cm^{-1}$. According to theory, these frequencies should correspond to intense absorption bands of the vibrational spectrum of gaseous CH_3Cl. In fact, the IR spectrum of gaseous CH_3Cl shows characteristic vibrational bands around $1015\,cm^{-1}$, assigned to its ν_6(e) CH_3 rocking mode. In contrast, none of the characteristic absorption bands of the CH_3Cl spectrum can account for $T_{iso} = 376 \pm 2\,K$ obtained for the F series. Rather, this T_{iso} value reflects the activation of the F ions by a more intimate mechanism involving their transient complexation with a CH_3Cl molecule. Indeed, HF/6–31G* calculations of a model complex between *O*-protonated benzyl methyl ether and CH_3Cl indicate the presence of nine vibrational frequencies over those characteristic of the two isolated components. Among these, that related to the out-of-plane C—Cl···H—O bending mode falls at $572\,cm^{-1}$, a value which is close to the experimental value $\omega_F = 523 \pm 3\,cm^{-1}$. The same $572\,cm^{-1}$ vibrational mode coincides with the critical $\omega_{diss} = 569\,cm^{-1}$ value for the dissociation of the E family ($T_{iso} = 409 \pm 5\,K$).

It is concluded that the inversion of configuration of the selected family of **II** obeys two different reaction dynamics driven by the activation dynamics from the bulk gas (CH_3Cl). Thus, if activation proceeds predominantly through a resonant energy exchange with the ν_6(e) = $1015\,cm^{-1}$ CH_3 rocking mode of the unperturbed molecule of the bath gas (CH_3Cl), the inversion reaction proceeds through the dynamically most accessible transition state involving unassisted C_α—O bond rupture (the G family). If, instead, activation involves the out-of-plane C—Cl···H—O bending vibration developed in the intimate encounter complex between CH_3Cl and **II**, the inversion reaction proceeds through the energetically most accessible transition state where the CH_3OH motion is assisted by coordination with the acidic hydrogens of the benzylic residue (the F family). The same vibrational mode is active in promoting the dissociation of most of **II** ions, irrespective of whether they belong to the F or G sets.

CONCLUSIONS

The advantages of studying INC in the gas phase instead of in a solvent cage come from the possibility of making precise statements about the factors governing their dynamics and reactivity in the lack of any perturbing environmental effects (solvation, ion pairing, cage viscosity, etc.). These effects may be evaluated by comparing

the behavior of INC in the gaseous phase with that of the same system in solution. An experimental methodology has been developed for this purpose, the result of which demonstrate that ionic processes in solution are mostly governed by the lifetime and the dynamics of intimate ion–neutral complexes and that these can in turn be profoundly influenced by the nature of the reaction medium. The results of the present study show for the first time the possible coexistence of different activation dynamics and their strict connection with the evolution dynamics and mechanism of INC in the gas phase. Competing processes in an INC can be promoted by the same activation dynamics, whereas the same process can be promoted by different activation dynamics depending on the nature of the INC involved.

Acknowledgments

The author thanks his collaborators and colleagues A. Filippi, G. Roselli, G. Renzi and F. Grandinetti for making the present research work possible. Thanks are also due to the Italian Ministero della Università e della Ricerca Scientifica e Tecnologica (MURST) and the Consiglio Nazionale delle Ricerche (CNR) of Italy for financial support.

REFERENCES

1. Morton TH. *Tetrahedron* 1982; **38**: 3195–3243.
2. Bowen RD. *Acc. Chem. Res.* 1991; **24**: 364–371.
3. Morton TH. *Org. Mass Spectrom.* 1992; **27**: 353–368.
4. McAdoo DJ, Morton TH. *Acc. Chem. Res.* 1993; **26**: 295–302.
5. Speranza M. In *Fundamentals and Applications of Gas Phase Ion Chemistry*, Jennings KR (ed). Kluwer: Dordrecht, 1999; 335–380.
6. Filippi A, Roselli G, Renzi G, Grandinetti F, Speranza M. *Chem. Eur. J.* 2003; **9**: 2072–2078.
7. Filippi A, Speranza M. *Chem. Eur. J.* 2003; **9**: 5274–5282.
8. Cacace F, Ciranni G, Giacomello P. *J. Am. Chem. Soc.* 1981; **103**: 1513–1516.
9. Linert W, Jameson RF. *Chem. Soc. Rev.* 1989; **18**: 477–505, and references cited therein.
10. Larsson R. *Catal. Today* 1988; **3**: 387–394.